Electronic Supplementary Material (ESI) for ChemComm.

Hydroxyl-enriched high-crystalline TiO_2 suspensible photocatalyst: Facile synthesis and superior H_2-generation activity

Duoduo Gao,[a] Jiachao Xu,[a] Huogen Yu,[a]* Yongping Liu,[b]* and Jiaguo Yu[c]

[a] State Key Laboratory of Silicate Materials for Architectures, Wuhan University of Technology, Wuhan, 430070, PR China

[b] Guangxi Key Laboratory of Electrochemical and Magneto-chemical Functional Materials, College of Chemistry and Bioengineering, Guilin University of Technology, Guilin 541004, PR China

[c] State Key Laboratory of Advanced Technology for Material Synthesis and Processing, Wuhan University of Technology, Wuhan 430070, PR China

Tel: 0086-27-87756662, Fax: 0086-27-87879468

E-mail: yuhuogen@whut.edu.cn (H.Yu); liuyp624@163.com (Y. Liu)

Supporting Information

EXPERIMENTAL SECTION

SI-1 Preparation and H_2-evolution tests of OH-enriched high-crystalline TiO_2 nanocrystal suspensible photocatalyst

The OH-enriched high-crystalline TiO_2 nanocrystal suspensible photocatalyst (suspensible TiO_2-NCs) were synthesized by a facile ethanol-controlled method, which includes simultaneous hydrolysis of ethanol-isolated tetrabutyl titanate ($Ti(OC_4H_9)_4$, TBOT) molecules in water and the following *in-situ* hydrothermal crystallization to produce suspensible TiO_2-NCs. First, 213 μL of TBOT was mixed with 20 mL of ethanol to form a clear and transparent TBOT-EtOH solution, where the volume ratio of TBOT to ethanol was regulated to be 1:94. Next, the above solution was directly and dropwise added into 60-mL deionized water and vigorously stirred for 0.5 h to obtain suspensible amorphous TiO_2 nanoparticle (suspensible TiO_2-NPs) photocatalyst. Subsequently, the attained suspensible TiO_2-NPs was transferred into a 100 mL of Teflon-sealed autoclave and maintained at 160 ^{o}C for 10 h. To characterize the morphology and microstructures (such as FESEM and TEM), the suspensible TiO_2-NCs and TiO_2-NPs were collected by centrifugation, washed with distilled water several times, and finally dispersed in ethanol by ultrasound. For the other characterizations (such as XRD, UV-vis, FTIR, XPS, BET, PL and photoelectrochemical analysis), the above suspensible TiO_2-NCs and TiO_2-NPs were filtrated, washed and dried at room temperature for 12 h to obtain the TiO_2-NCs and

TiO_2-NPs powder sample. For the photocatalytic H_2-evolution experiment of suspensible TiO_2-NCs and TiO_2-NPs photocatalyst, the above suspension solution was directly applied for the subsequent H_2-evolution test, and the subsequent details are exhibited in section of **SI-4 Photocatalytic tests**.

To explore the impact of ethanol content on the suspendability of TiO_2-NCs photocatalyst, the volume ratio of TBOT to ethanol was regulated to be 1:0, 1:10, 1:50, 1:70 and 1:94, and the obtained product were showed in Fig. 1C.

SI-2 Traditional preparation of amorphous and crystalline TiO_2 aggregates photocatalyst

The traditional crystalline TiO_2 aggregates (crystalline TiO_2-AGs) were synthesized by a simple hydrolysis-calcination method. Briefly, 1 mL of tetrabutyl titanate ($Ti(OC_4H_9)_4$, TBOT) was directly added into 80 mL of deionized water for the effective hydrolysis to produce amorphous TiO_2 aggregates (amorphous TiO_2-AGs). After continuously stirring for 0.5 h, the obtained white precipitate was washed and dried. The above powder was further calcined at 550 ^oC for 4 h to obtain the crystalline TiO_2-AGs photocatalyst.

SI-3 Characterization

A JEM-2100F transmission electron microscope (TEM) and a JSM-7500F field emission scanning electron microscope (FESEM) were applied to detect the structure and morphology of prepared samples. The crystal structure was demonstrated on a

Rigaku III X-ray diffractometer (XRD). To analyze the chemical state of samples, a KRATOA XSAM800 system (XPS) was used. TG-DSC results were obtained by employing integrated thermal analyzer (STA449F3, Germany). The UV-2450 spectrophotometer was applied to record UV-Vis absorption spectra. The PL spectra and carrier lifetime were analyzed by FLS920 with 365-nm light source.

SI-4 Photocatalytic tests

The H_2-production rate of various photocatalysts was investigated under UV light irradiation. Typically (in addition to the suspensible photocatalysts), the photocatalysts (50 mg) were dispersed in 80-mL ethanol solution (25 vol%) to produce a homogeneous suspension. Subsequently, nitrogen was purged into the above system for 15 min to create an anaerobic environment, and four 365-nm LEDs (3W, 42 mW/cm^2) were selected as the irradiation source. The H_2-generation amount is measured by gas chromatograph (GC-2014C, Shimadzu, TCD, Japan).

SI-5 Photoelectrochemical performance

The photoelectrochemical properties were studied via employing a three-electrode CHI660E electrochemical apparatus in a Na_2SO_4 electrolyte (0.5 M) with FTO glass (loading with photocatalysts), saturated calomel electrode and Pt plate as working electrode, reference electrode and counter electrode, respectively. The anaerobic system can be produced via aerating with nitrogen and the LED irradiator (365-nm, 3 W) as light source. The above working electrode can be fabricated via dropping the sample mixed slurry containing 10 mg photocatalyst and a solution of D-520 Nafion and ethanol (1:1 in volume ratio) onto the substrate of FTO. The *i-t* curve can be achieved with the UV light repeated ON/OFF at a set time period of 60 s. The EIS was carried out in 10^{-3} Hz-1000 KHz (frequency). In addition, the bias voltages (−0.8 to −1.4 V) were previously fixed to measure the LSV.

SI-6 The AQE calculation

The apparent quantum efficiency (AQE) of suspensible TiO_2-NCs photocatalyst is calculated via the following equation:

$$\begin{aligned}\mathrm{AQE}(\%) &= \frac{\text{number of reacted electrons}}{\text{number of incident photons}} \times 100\% \\ &= \frac{\text{number of evolved } \mathrm{H_2} \text{ molecules} \times 2}{\text{number of incident photons}} \times 100\%\end{aligned}$$

The total power of the UV light (four 3-W 365 nm) was 42 mW/cm^2, which was detected by an irradiatometer (UV-B, Beijing Normal University Optical Instrument). Hence, the AQE can be calculated to be 2.1 %.

Table S1. Composition (at%) of the various samples according to XPS analysis

Samples	Ti-O	-OH
suspensible TiO_2-NPs	55.95	44.05
suspensible TiO_2-NCs	56.40	43.60
amorphous TiO_2-AGs	100	0
crystalline TiO_2-AGs	100	0

Table S2. Fluorescence Emission Lifetime and Relevant Percentage Data Fitted by a Three-Exponential Function

Samples	τ_1 (ns)	A_1 (%)	τ_2 (ns)	A_2 (%)	τ_3 (ns)	A_3 (%)	Average lifetime (τ_a) (ns)	χ^2
suspensible TiO_2-NPs	0.29	39.36	2.66	42.87	11.41	17.77	7.98	1.14
suspensible TiO_2-NCs	0.30	17.08	2.62	51.77	11.17	31.15	8.68	1.08
crystalline TiO_2-AGs	0.59	25.38	3.16	55.84	12.44	18.78	8.17	1.06

The fitted parameters are acquired via the following tri-exponential formulas:

$$I_{(t)} = I_0 + A_1\exp(-t/\tau_1) + A_2\exp(-t/\tau_2) + A_3\exp(-t/\tau_3) \quad (1)$$

$$\tau_a = (A_1\tau_1^2 + A_2\tau_2^2 + A_3\tau_3^2)/(A_1\tau_1 + A_2\tau_2 + A_3\tau_3) \quad (2)$$

where I_0 is the baseline correction value, A_1, A_2 and A_3 represent the tri-exponential factors, and τ_1, τ_2, τ_3 and τ_a corresponding the lifetime in various stages (radiation, non-radiation and energy transfer) and average lifetime, χ^2 is the goodness-of-fit.

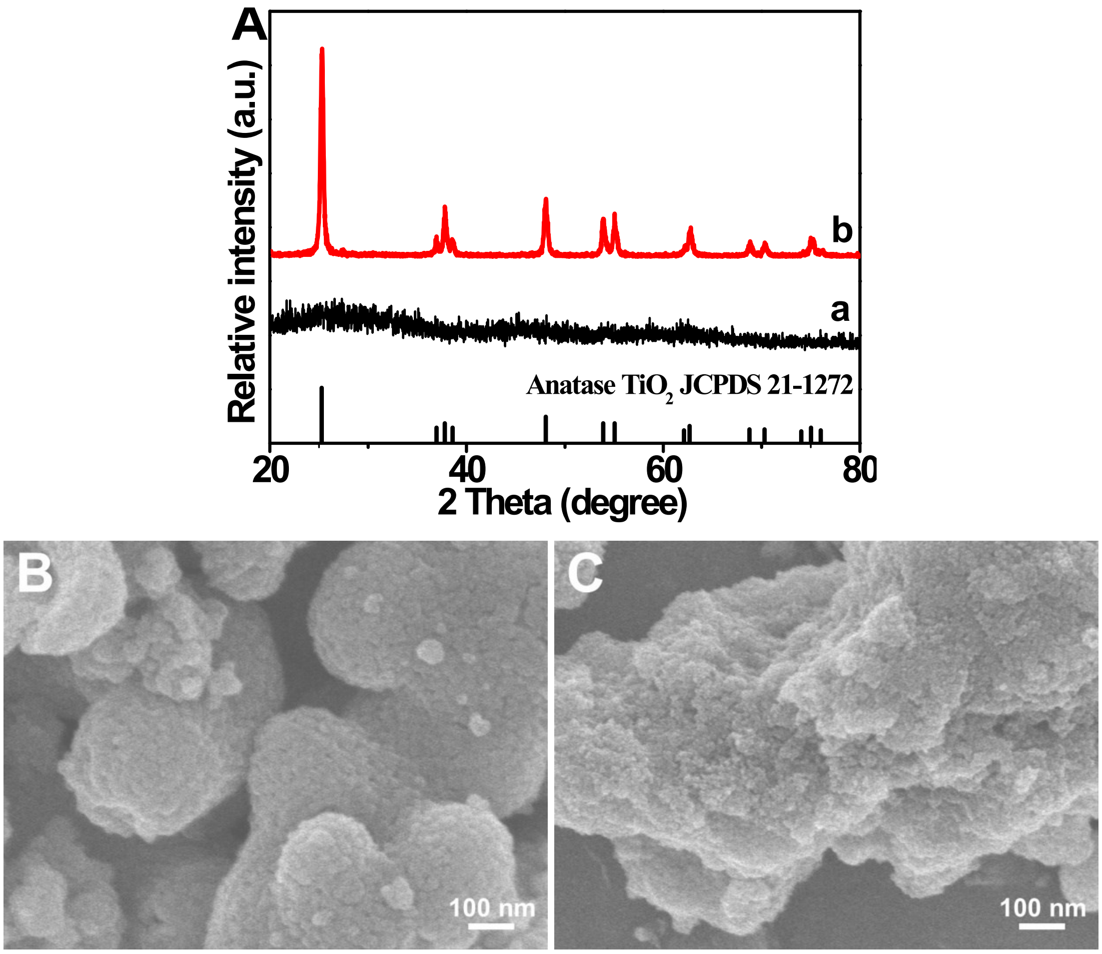

Fig. S1 (A) XRD patterns of (a) conventional amorphous TiO_2-AGs and (b) conventional crystalline TiO_2-AGs; (B, C) FESEM images of (B) conventional amorphous TiO_2-AGs and (C) conventional crystalline TiO_2-AGs.

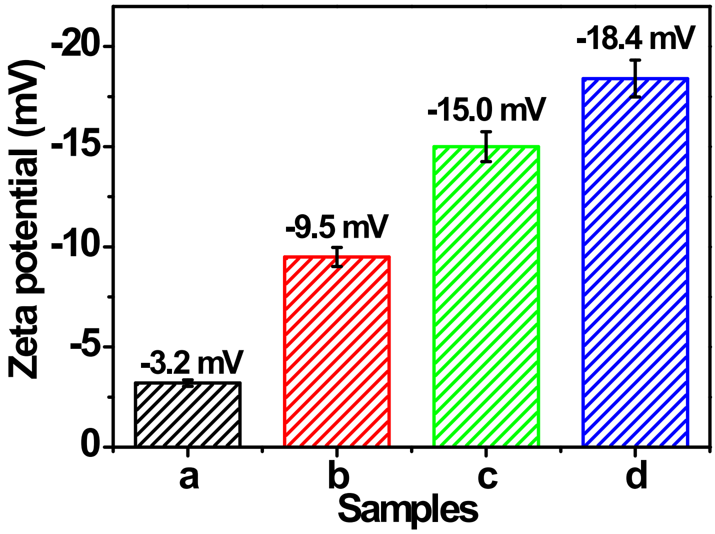

Fig. S2 Zeta potentials of various TiO_2 samples with different $V_{(ethanol)}$: $V_{(TBOT)}$: (a) 0:1, (b) 10:1, (c) 50:1 and (e) 94:1.

The Zeta potentials of various TiO_2 photocatalysts (obtained with different $V_{(ethanol)}$: $V_{(TBOT)}$) were measured, as shown in Fig. S2. Obviously, all the resultant TiO_2 samples display the negative potential due to the *in-situ* produced hydroxyl groups (with the negative charges). In addition, the absolute value of Zeta potential increased with increasing ethanol amount in precursor solution, which can be primarily attributed to the increase of surface OH amount, clearly suggesting that the amount of surface OH can be effectively controlled by regulating the volume ratio of ethanol to TBOT. The above results also manifest that ethanol plays a key role for the synthesis of hydroxyl-enriched suspensible TiO_2-NCs photocatalyst.

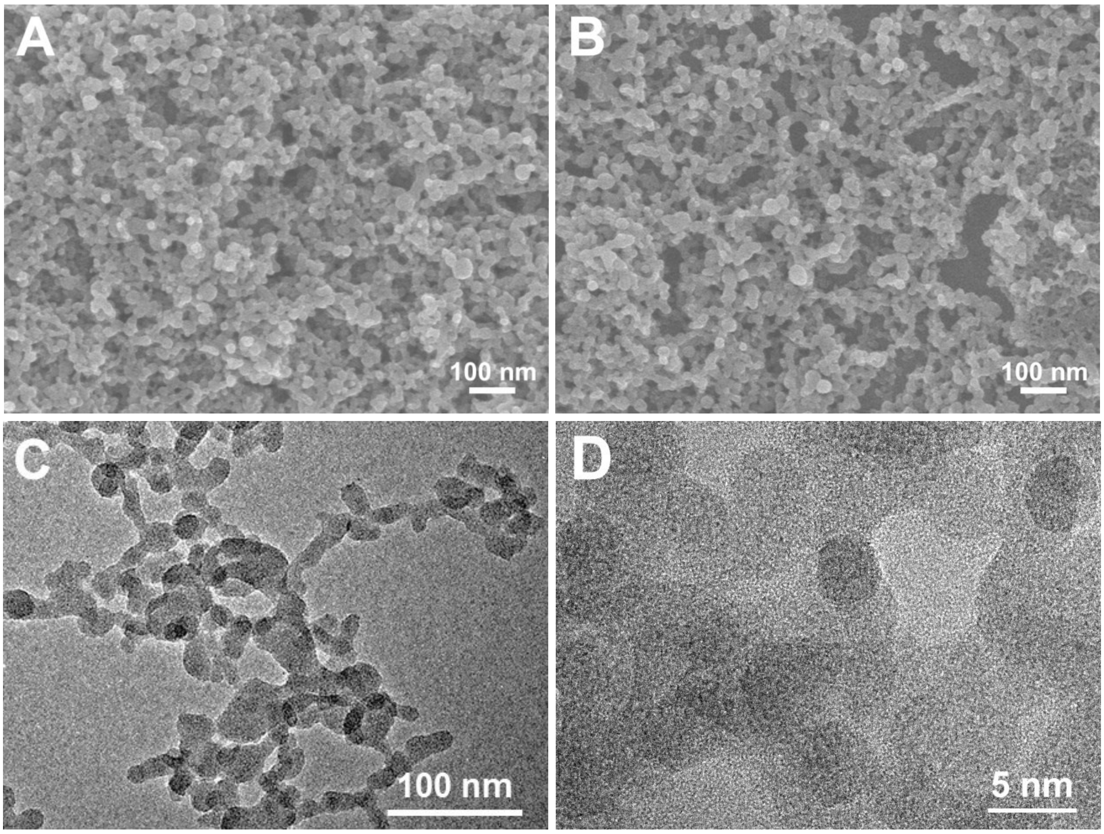

Fig. S3 (A, B) FESEM images of (A) suspensible TiO_2-NPs and (B) suspensible TiO_2-NCs; (C, D) typical TEM images of suspensible TiO_2-NPs.

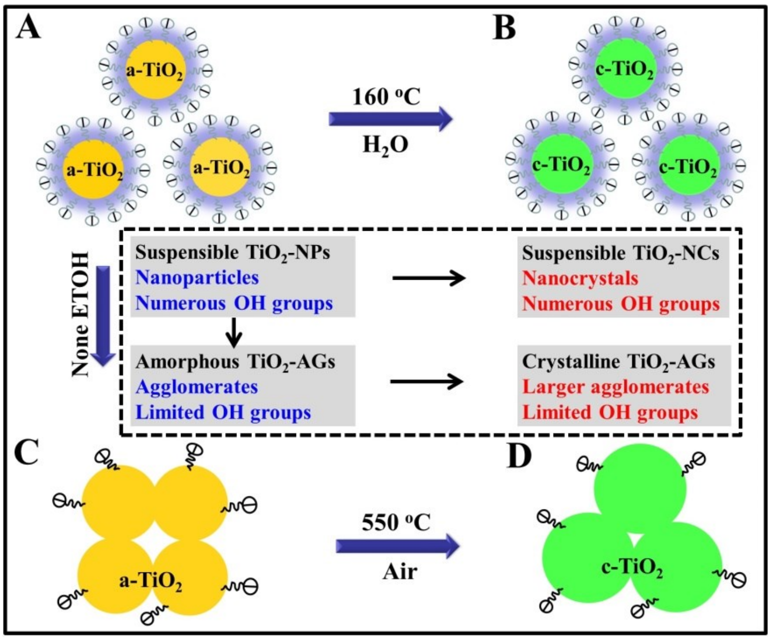

Fig. S4 Different TiO_2 photocatalysts with OH groups: (A) suspensible TiO_2-NPs, (B) suspensible TiO_2-NCs, (c) conventional amorphous TiO_2-AGs, and (D) conventional crystalline TiO_2-AGs.

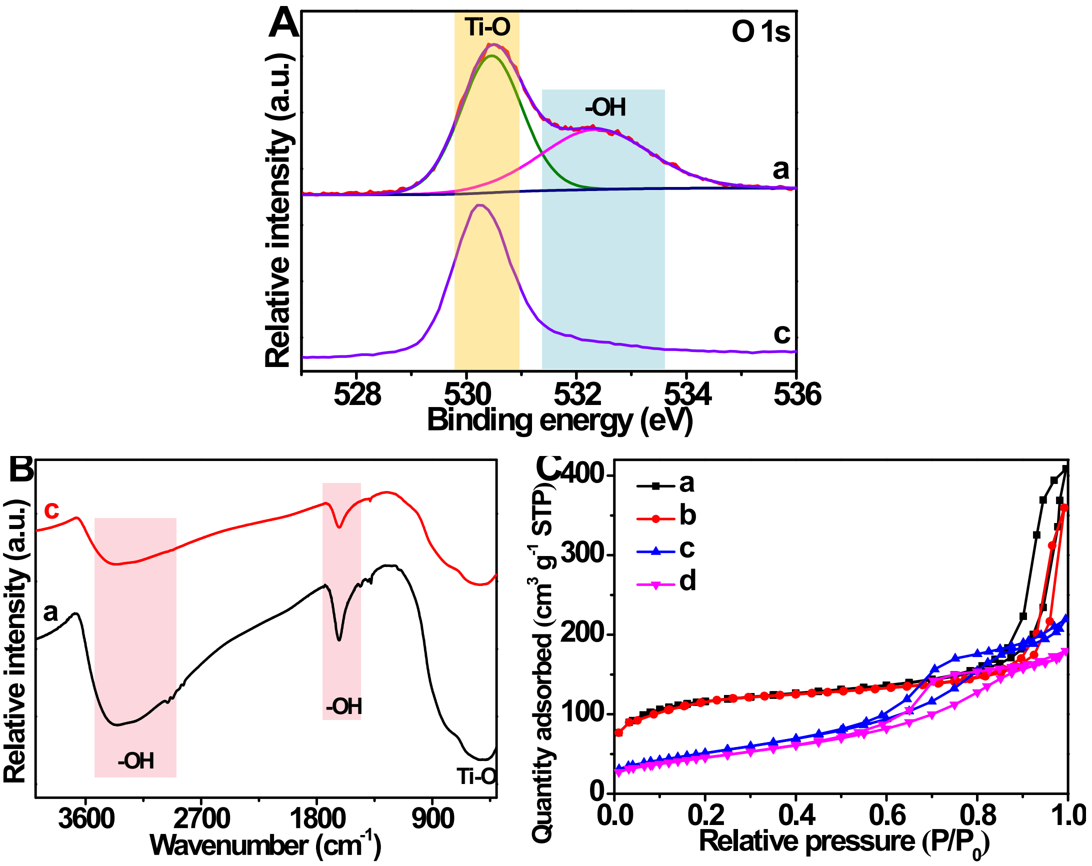

Fig. S5 (A) High-resolution XPS spectra of O 1*s*; (B) FTIR and (C) BET results for various samples: (a) suspensible TiO_2-NPs, (b) suspensible TiO_2-NCs, (c) conventional amorphous TiO_2-AGs and (d) conventional crystalline TiO_2-AGs.

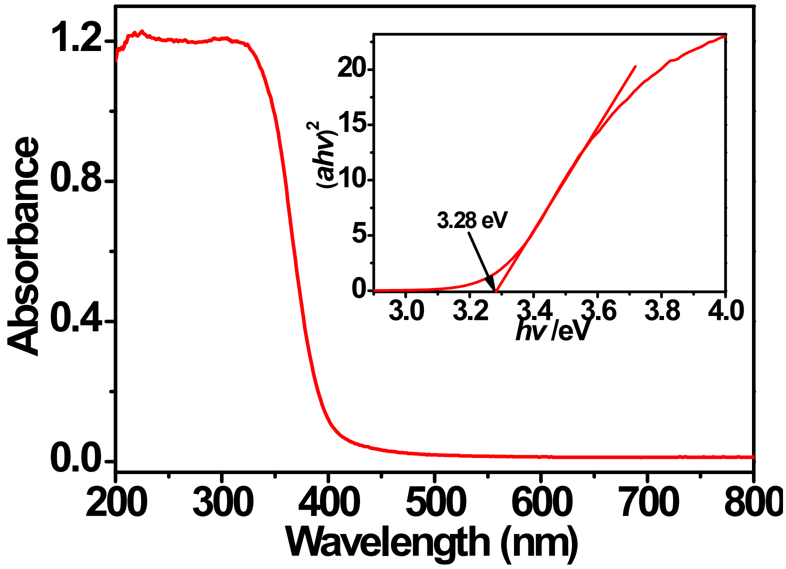

Fig. S6 UV-vis spectra and its calculated band gap (inset) of suspensible TiO_2-NCs.

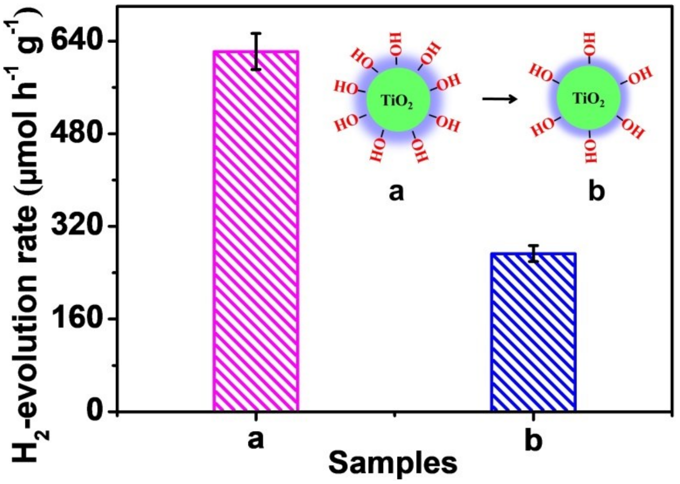

Fig. S7 Comparison of photocatalytic H_2-evolution activity for various samples: (a) OH-enriched suspensible TiO_2-NCs, and (b) dried TiO_2-NCs.

To further investigate the significant effect of the OH-enriched surface on the photocatalytic performance of the suspensible TiO_2-NCs photocatalyst, the suspensible TiO_2-NCs were separated, washed and dried at room temperature. The resulting dried TiO_2-NCs sample clearly exhibits a larger aggregate due to the obvious reduction of hydroxyl groups on the TiO_2-NCs surface (Fig. 1D-g). In this case, the present dried TiO_2-NCs sample displays a noticeably declined H_2-production activity (Fig. S7). Hence, the above results strongly reveal that the enriched hydroxyl groups are quite essential for photocatalytic H_2-evolution, which can not only maintain the excellent suspensibility of the TiO_2-NCs, but also act as the active sites for TiO_2 to dramatically boost its photocatalytic H_2-evolution rate.

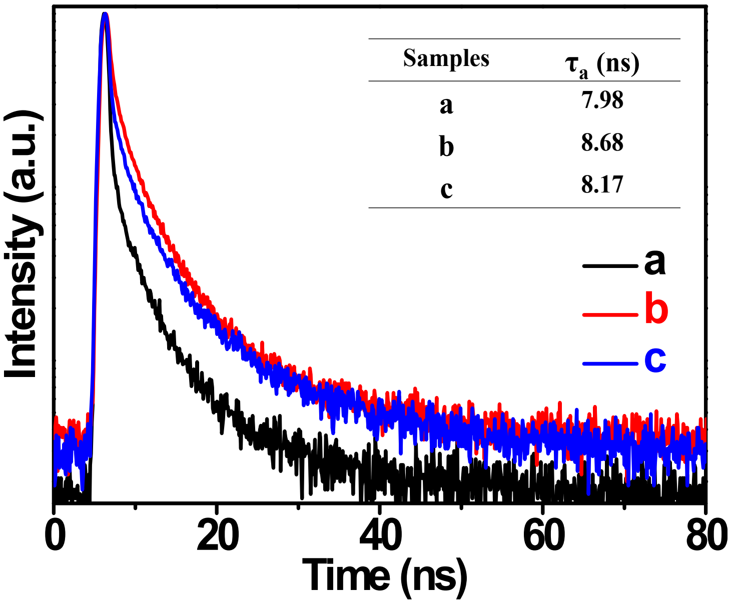

Samples	τ_a (ns)
a	7.98
b	8.68
c	8.17

Fig. S8 Transient-state photoluminescence spectras for various samples: (a) suspensible TiO_2-NPs, (b) suspensible TiO_2-NCs and (c) conventional crystalline TiO_2-AGs.

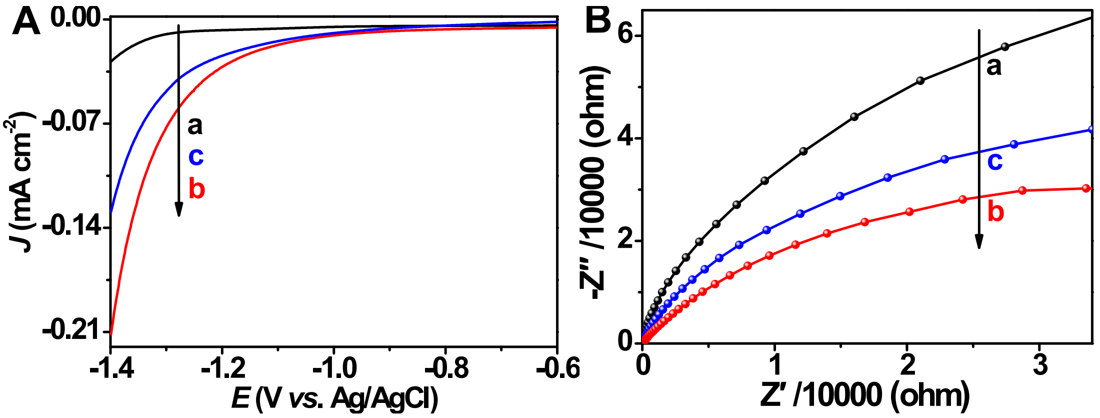

Fig. S9 (A) LSV curves and (B) EIS curves for various samples: (a) suspensible TiO_2-NPs, (b) suspensible TiO_2-NCs, and (c) conventional crystalline TiO_2-AGs.